Human Molecular Genetics, 2013, Vol. 22, No. 25 ***5121–5135***
doi:10.1093/hmg/ddt366
Advance Access published on August 1, 2013

A comprehensive molecular study on Coffin–Siris and Nicolaides–Baraitser syndromes identifies a broad molecular and clinical spectrum converging on altered chromatin remodeling

Dagmar Wieczorek[1,*], Nina Bögershausen[4,5,6], Filippo Beleggia[4,5,6], Sabine Steiner-Haldenstätt[1], Esther Pohl[4,5,6], Yun Li[4,5,6], Esther Milz[4,5,6], Marcel Martin[8], Holger Thiele[7], Janine Altmüller[7], Yasemin Alanay[9,10], Hülya Kayserili[11], Ludger Klein-Hitpass[2,3], Stefan Böhringer[12], Andreas Wollstein[13], Beate Albrecht[1], Koray Boduroglu[10], Almuth Caliebe[14], Krystyna Chrzanowska[15], Ozgur Cogulu[16], Francesca Cristofoli[18], Johanna Christina Czeschik[1], Koenraad Devriendt[18], Maria Teresa Dotti[19], Nursel Elcioglu[21], Blanca Gener[22], Timm O. Goecke[23], Małgorzata Krajewska-Walasek[15], Encarnación Guillén-Navarro[24], Joussef Hayek[25], Gunnar Houge[26], Esra Kilic[10], Pelin Özlem Simsek-Kiper[10], Vanesa López-González[24], Alma Kuechler[1], Stanislas Lyonnet[27], Francesca Mari[20,37], Annabella Marozza[37], Michèle Mathieu Dramard[28], Barbara Mikat[1], Gilles Morin[28], Fanny Morice-Picard[29], Ferda Özkinay[17], Anita Rauch[30], Alessandra Renieri[20,37], Sigrid Tinschert[31,32], G. Eda Utine[10], Catheline Vilain[33], Rossella Vivarelli[34], Christiane Zweier[35], Peter Nürnberg[5,6,7], Sven Rahmann[36], Joris Vermeesch[18], Hermann-Josef Lüdecke[1], Michael Zeschnigk[1] and Bernd Wollnik[4,5,6]

[1]Institut für Humangenetik and, [2]Institut für Zellbiologie (Tumorforschung), Universitätsklinikum Essen and [3]Universität Duisburg-Essen, Essen, Germany, [4]Institute of Human Genetics, [5]Center for Molecular Medicine Cologne (CMMC), [6]Cologne Excellence Cluster on Cellular Stress Responses in Aging-Associated Diseases (CECAD) and [7]Cologne Center for Genomics (CCG), University of Cologne, Cologne, Germany, [8]Bioinformatics, Computer Science XI, TU Dortmund, Dortmund, Germany, [9]Department of Pediatrics, School of Medicine, Acibadem University, Istanbul, Turkey, [10]Department of Pediatric Genetics, Ihsan Dogramaci Children's Hospital, Hacettepe University School of Medicine, Ankara, Turkey, [11]Medical Genetics Department, Istanbul Medical Faculty, Istanbul University, Istanbul, Turkey, [12]Medical Statistics and Bioinformatics, Leiden University Medical Center, Leiden, The Netherlands, [13]Section of Evolutionary Biology, Department of Biology II, University of Munich LMU, Planegg-Martinsried, Germany, [14]Institut für Humangenetik, Christian-Albrechts-Universität zu Kiel, Kiel, Germany, [15]Department of Medical Genetics, The Children's Memorial Health Institute, Warsaw, Poland, [16]Department of Pediatric Genetics and [17]Department of Medical Genetics, Department of Pediatrics, Faculty of Medicine, Ege University, Izmir, Turkey, [18]Department of Human Genetics, Katholieke Universiteit Leuven, Leuven, Belgium, [19]Department of Medical Surgical and Neurological Sciences, Neurodegenerative Disease Unit, University of Siena, Siena, Italy, [20]Medical Genetics Unit, Medical Biotechnology Department, University of Siena, Siena, Italy, [21]Department of Pediatric Genetics, Marmara University Hospital, Istanbul, Turkey, [22]Department of Genetics, Hospital Universitario Cruces, Vizcaya, Spain, [23]Institut für Humangenetik, Universitätsklinikum Düsseldorf, Düsseldorf, Germany, [24]Medical Genetics Unit, Department of Pediatrics, Hospital Clínico Universitario Virgen de la Arrixaca, Murcia, Spain, [25]Child Neuropsychiatry Unit, University Hospital, AOUS, Siena, Italy, [26]Center for Medical Genetics and Molecular Medicine, Haukeland University Hospital, Bergen, Norway, [27]Department of Genetics, Université Paris Descartes – Sorbonne Paris Cité, Institut Imagine, Hôpital Necker-Enfants

[*]To whom correspondence should be addressed at: Institut für Humangenetik, Universitätsklinikum Essen, Universität Duisburg-Essen, Hufelandstr. 55, 45122 Essen, Germany. Tel: +49 201 723 4560; Fax: +49 201 723 5900; Email: dagmar.wieczorek@uni-due.de

© The Author 2013. Published by Oxford University Press. All rights reserved.
For Permissions, please email: journals.permissions@oup.com

Downloaded from https://academic.oup.com/hmg/article/22/25/5121/575160 by guest on 15 March 2022

Malades APHP, Paris, France, [28]Département de génétique médicale, CHRU Amiens, France, [29]Département de Génétique, CHU Bordeaux et Université de Bordeaux, Bordeaux, France, [30]Institute of Medical Genetics, University of Zurich, Schwerzenbach-Zurich, Switzerland, [31]Institut für Klinische Genetik, Technische Universität Dresden, Dresden, Germany, [32]Division of Human Genetics, Medical University Innsbruck, Austria, [33]Department of Medical Genetics, ULB Center of Human Genetics, Erasme Hospital, Brussels, Belgium, [34]Clinica Pediatrica, Policlinico Senese Le Scotte Viale Bracci, Siena, Italy, [35]Institut für Humangenetik, Friedrich-Alexander-Universität Erlangen-Nürnberg, Erlangen, Germany, [36]Genome Informatics, Institute of Human Genetics, Faculty of Medicine, University of Duisburg-Essen, Essen, Germany and [37]Genetica Medica, Azienda Ospedaliera Universitaria Senese, Siena, Italy

Received May 30, 2013; Revised July 25, 2013; Accepted July 26, 2013

Chromatin remodeling complexes are known to modify chemical marks on histones or to induce conformational changes in the chromatin in order to regulate transcription. *De novo* dominant mutations in different members of the SWI/SNF chromatin remodeling complex have recently been described in individuals with Coffin–Siris (CSS) and Nicolaides–Baraitser (NCBRS) syndromes. Using a combination of whole-exome sequencing, NGS-based sequencing of 23 SWI/SNF complex genes, and molecular karyotyping in 46 previously undescribed individuals with CSS and NCBRS, we identified a *de novo* 1-bp deletion (c.677delG, p.Gly226Glufs*53) and a *de novo* missense mutation (c.914G>T, p.Cys305Phe) in *PHF6* in two individuals diagnosed with CSS. PHF6 interacts with the nucleosome remodeling and deacetylation (NuRD) complex implicating dysfunction of a second chromatin remodeling complex in the pathogenesis of CSS-like phenotypes. Altogether, we identified mutations in 60% of the studied individuals (28/46), located in the genes *ARID1A, ARID1B, SMARCB1, SMARCE1*, *SMARCA2,* and *PHF6*. We show that mutations in *ARID1B* are the main cause of CSS, accounting for 76% of identified mutations. *ARID1B* and *SMARCB1* mutations were also found in individuals with the initial diagnosis of NCBRS. These individuals apparently belong to a small subset who display an intermediate CSS/NCBRS phenotype. Our proposed genotype-phenotype correlations are important for molecular screening strategies.

INTRODUCTION

The transcription of the human genome is an intricately regulated process that relies on many contributing factors. There are numerous known multiprotein complexes, which act by addition or removal of chemical marks on histones or by induction of conformational chromatin changes in order to fine-tune the transcriptional control of specific genes in specific cellular contexts or at defined time points in development. In the past few years, several of these so-called "chromatin remodeling complexes" have been implicated in the pathogenesis of developmental disorders. Among these is the SWI/SNF complex, a chromatin remodeling complex that mainly functions through nucleosome mobilization, thereby increasing the accessibility of promoters to DNA-binding proteins (1). Very recently, mutations in the genes *ARID1A, ARID1B, SMARCA4, SMARCB1* and *SMARCE1*, all of them encoding proteins belonging to the SWI/SNF complex, were identified to be causative of Coffin–Siris syndrome (CSS, MIM 135900) (2,3). Interestingly, truncating mutations in *ARID1B* have also been described in individuals with unspecific intellectual disability (ID) (4). CSS is a rare congenital disorder that is characterized by a combination of hypoplasia/aplasia of the fifth digit or finger-/toenail, ID and facial coarseness with a wide mouth with thick, everted upper and lower lips, a broad nasal bridge and nasal tip, thick eyebrows and long eyelashes. Additionally, there may be organ malformations, hirsutism, sparse scalp hair, short stature and microcephaly of variable degrees (5–7). Mutations in the SWI/SNF complex member *SMARCA2* were described to underlie Nicolaides–Baraitser syndrome in 2012 (8). Nicolaides–Baraitser syndrome (NCBRS, MIM 601358), first described in 1993, is characterized by severe ID, seizures, short stature, microcephaly, facial coarseness and sparse hair (9). Notably, NCBRS individuals do not display hypoplasia of digits but a swelling of interphalangeal joints as a distinctive feature (10).

Using a combination of whole-exome sequencing, NGS-based sequencing of 23 SWI/SNF complex genes, and molecular karyotyping in 46 undescribed individuals with a clinical diagnosis of either CSS or NCBRS, we add *PHF6* as a causative gene for the CSS phenotypic spectrum and show that mutations in *ARID1B* are the main cause of CSS. *ARID1B* mutations can also be found in individuals clinically diagnosed with NCBRS, suggesting that these syndromes might represent a phenotypic spectrum rather than two distinct disorders.

RESULTS

PHF6 mutations in female individuals diagnosed with CSS

Whole-exome sequencing was performed in individual K2436. She presented with mild-to-moderate developmental delay, hypertrichosis, coarse facial features, a-/hypoplastic fifth finger- and toenail, and hypoplastic fifth digit and fulfilled the diagnostic criteria for CSS (Fig. 1A; Tables 2 and 3) (6). No causative variant was detected in any of the described CSS genes. Searching for *de novo* mutations identified a c.914G>T

Downloaded from https://academic.oup.com/hmg/article/22/25/5121/575160 by guest on 15 March 2022

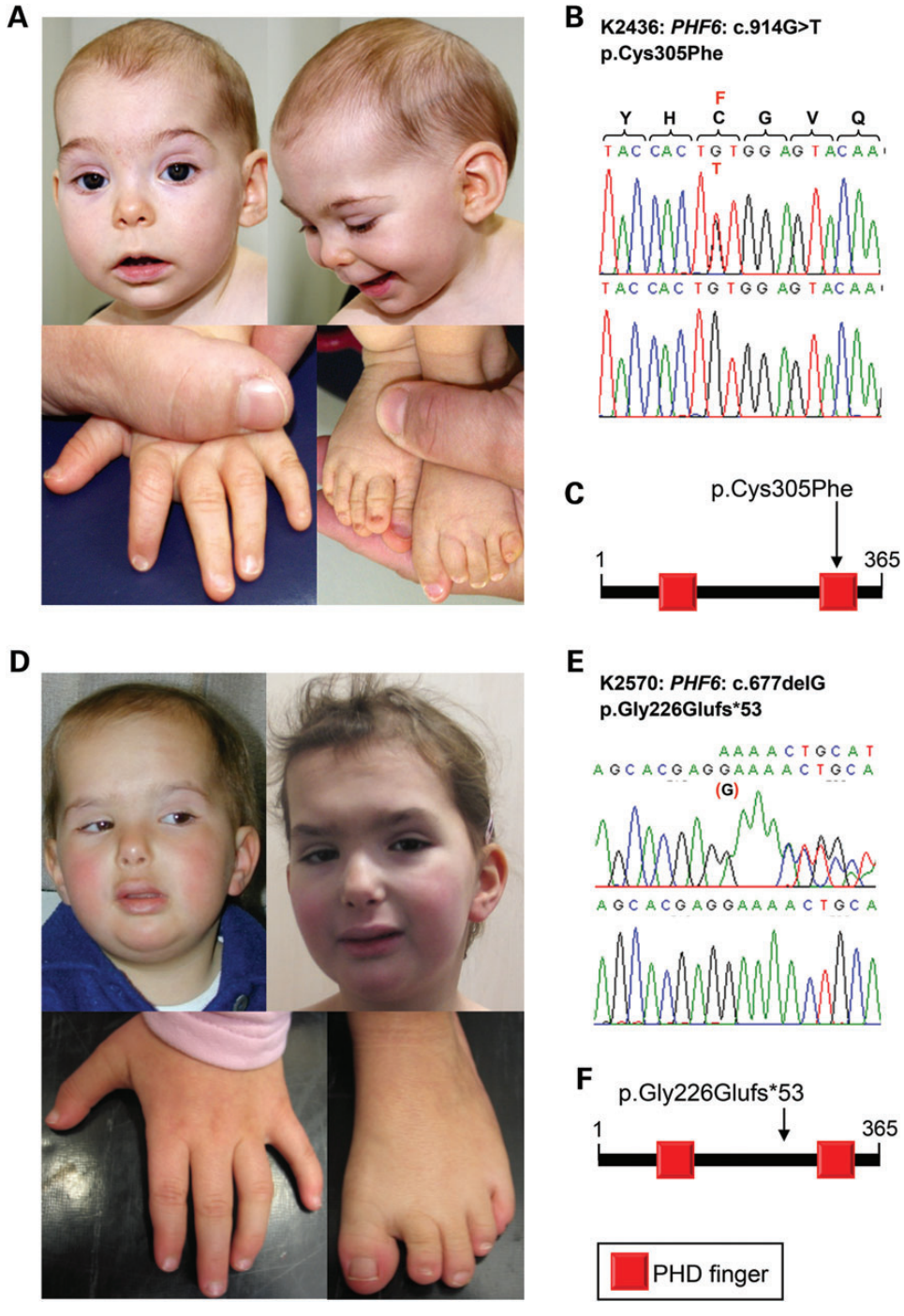

Figure 1. Phenotype of females with *PHF6* mutation. (**A**)Individual K2436 at the age of 12 months with sparse hair, pointed eyebrows with synophrys, long philtrum, thin upper and thick lower vermillion border. Hypoplasia of the fifth fingernail, short toes with hypoplastic fifth toenail. (**B**) Electropherogram of the *PHF6* missense mutation identified in individual K2436 compared to wildtype. (**C**) Schematic representation of the PHF6 protein; the p.Cys305Phe mutation is located within the second PHD finger domain. (**D**) Individual K2570 at the age of 2 and 3 years with full eyebrows, synophrys, short philtrum and full lips. Brachytelephalangy and hypoplastic nails of all fingers as well as brachydactyly of toes and hypoplastic fifth toenail. (**E**)Electropherogram of the *PHF6* frameshift mutation identified in individual K2570 compared with wildtype. (**F**)Schematic representation of the PHF6 protein; the p.Gly226Glufs*53 mutation is 13 amino acid upstream of the second PHD finger domain.

substitution in *PHF6,* a gene located within Xq26.3. Sanger sequencing confirmed *de novo* occurrence. The substitution affects a conserved cysteine at position 305 within the second PHD finger domain of the protein (p.Cys305Phe; Fig. 1B and C, Table 1), and is predicted to be probably damaging with a score of 0.997 by PolyPhen (http://genetics.bwh.harvard.edu/pph2/).

We screened additional nine female and nine male individuals with typical clinical findings of CSS who were negative for mutations within the described SWI/SNF complex genes for

Downloaded from https://academic.oup.com/hmg/article/22/25/5121/575160 by guest on 15 March 2022

Table 1. Overview of identified mutations

Individual	Referral diagnosis	Gene	Exon	cDNA	Protein	Inheritance
K2570	CSS	*PHF6*	7	c.677delG	p.Gly226Glufs*53	*De novo*
K2436*	CSS	*PHF6*	9	c.914G>T	p.Cys305Phe	*De novo*
K2437*	CSS	*ARID1B*	1	c.1540dupC	p.Gln514Profs*21	*De novo*
K2574	CSS	*ARID1B*	4	c.1808dupG	p.Ser603Argfs*50	*De novo*
K2434*	CSS	*ARID1B*	6	c.2248C>T	p.Arg750*	*De novo*
K2441	CSS	*ARID1B*	6	c.2248C>T	p.Arg750*	*De novo*
K2474	CSS	*ARID1B*	9	c.2692C>T	p.Gln898*	*De novo*
K2471	CSS	*ARID1B*	9	c.2723delC	p.Pro908Hisfs*6	*De novo*
K2445	CSS	*ARID1B*	18	c.4216_4217insTGCTGCTGCTCCTACTCGG	p.Gln1406Leufs*59	*De novo*
K2444	CSS	*ARID1B*	18	c.4770_4771delinsG	p.Gln1591Argfs*23	*De novo*
K2439	CSS	*ARID1B*	20	c.5071delC	p.Leu1691*	n.a.
K2432	CSS	*ARID1B*	20	c.5457G>A	p.Trp1819*	n.a.
K2578	CSS	*ARID1B*	20	c.6041G>A	p.Trp2014*	n.a.
K2583	CSS	*ARID1B*	20	c.6041G>A	p.Trp2014*	n.a.
K2443	CSS	*ARID1B*	20	c.6382C>T	p.Arg2128*	*De novo*
K2693	CSS	*ARID1B*	20	c.6439dupA	p.Arg2147Lysfs*45	*De novo*
K2428	CSS	*ARID1B*		arr[hg19] 6q25.3(157,402,040–157,460,542)x1		*De novo*
K2438	CSS	*ARID1B*		arr[hg19] 6q25.3(156,960,439–158,889,653)x1		*De novo*
K2435*	CSS	*ARID1A*	20	c.5965C>T	p.Arg1989*	*De novo*
K2426*	CSS	*SMARCB1*	9	c.1121G>A	p.Arg374Gln	*De novo*
K2442*	CSS	*SMARCE1*	5	c.218A>C	p.Tyr73Ser	*De novo*
K2587	NCBRS	*ARID1B*	4	c.1871delC	p.Pro624Hisfs*44	*De novo*
K2586	NCBRS	*ARID1B*	12	c.3430C>T	p.Gln1144*	n.a.
K2705	NCBRS	*ARID1B*	14	c.3586dupC	p.Gln1196Profs*14	*De novo*
K2588	NCBRS	*SMARCB1*	8	c.1096C>T	p.Arg366Cys	*De novo*
K2703	NCBRS	*SMARCA2*	18	c.2554G>A	p.Glu852Lys	*De novo*
K2704	NCBRS	*SMARCA2*	18	c.2639C>T	p.Thr880Ile	*De novo*
K2706	NCBRS	*SMARCA2*	18	c.2564G>A	p.Arg855Gln	*De novo*

*, Discovery cohort (exome); n.a, parental samples unavailable; CSS = Coffin–Siris syndrome; NCBRS, Nicolaides–Baraitser syndrome

mutations in *PHF6* and could identify a *de novo* truncating mutation (c.677delG; p.Gly226Glufs*53) in individual K2570 (Fig. 1D–F). For one remaining patient (K2707), no DNA was available for *PHF6* sequencing.

Mutational spectrum of the SWI/SNF complex

Whole-exome sequencing in three severely affected (K2426, K2437, K2442) and two mildly affected individuals with CSS (K2434, K2435) revealed causative mutations in four of them: truncating mutations in *ARID1A* (K2435; Fig. 2A–C) and *ARID1B* (K2434) and missense mutations in *SMARCB1* (K2426; Fig. 2D–F) and *SMARCE1* (K2442; Fig. 2G–I) (Table 1). The mutant allele in the *ARID1A* mutation carrier was detected in a lower proportion than the wild-type allele, indicating the presence of somatic mosaicism in the individual (Fig. 2B). Initially, we missed the truncating mutation in *ARID1B* in individual K2437 due to insufficient coverage of exon 1 of the *ARID1B* gene, but identified the mutation later by Haloplex enrichment followed by next-generation sequencing. Parental DNA was finally available for all five affected individuals and the mutations were proven to be *de novo*.

The *de novo* missense mutation p.Arg374Gln in *SMARCB1* is located within exon 9 of the gene and leads to the substitution of an evolutionary highly conserved amino acid in close proximity of the sucrose non-fermenting domain 5 (SNF5) of the protein, likely affecting domain structure (Fig. 2E and F). All seven mutations within this gene previously described in individuals with a CSS phenotype are located in exons 8 and 9 of the *SMARCB1* gene (3,11). In addition, PolyPhen (http://genetics.bwh.harvard.edu/pph2/) predicts this variant to be probably damaging with a score of 0.998. The *de novo SMARCE1* missense mutation p.Tyr73Ser in individual K2442 is the second mutation described in this gene, so far. It affects the same highly conserved amino acid at position 73 within the high mobility domain (HMG box) of the protein as the mutation described by Tsurusaki *et al*.(3), but causes a change of tyrosine to serine instead to cysteine (2 Fig. 2H and I). PolyPhen (http://genetics.bwh.harvard.edu/pph2/) predicts this change to be probably damaging with a score of 0.990.

Using massive parallel sequencing of 23 genes enriched by the Haloplex technology followed by next-generation sequencing, we found 12 putatively pathogenic sequence variants in genes associated with the SWI/SNF complex in 13 of 32 individuals (41%) with a diagnosis of CSS (Table 1, Supplementary Material, Fig. S6). All of the identified mutations were novel loss-of-function mutations in *ARID1B*, either base substitutions or small insertions/deletions that lead immediately or after a frame-shift to premature stop codons. Using the Pindel program (12) in order to detect larger insertions/deletions, we identified a 19-bp insertion in *ARID1B* in one individual. Parental DNA was available for 10 individuals with a truncating *ARID1B* mutation and in these individuals, the mutations were proven to be *de novo*. The p.Trp2014* in exon 20 was found twice and the p.Arg750* identified in an individual from the discovery cohort was found in an additional individual. One putative missense mutation in *ARID1A* (c.358C>T, p.P120S) was found in an individual with CSS for whom no parental DNA was available. However, this

Downloaded from https://academic.oup.com/hmg/article/22/25/5121/575160 by guest on 15 March 2022

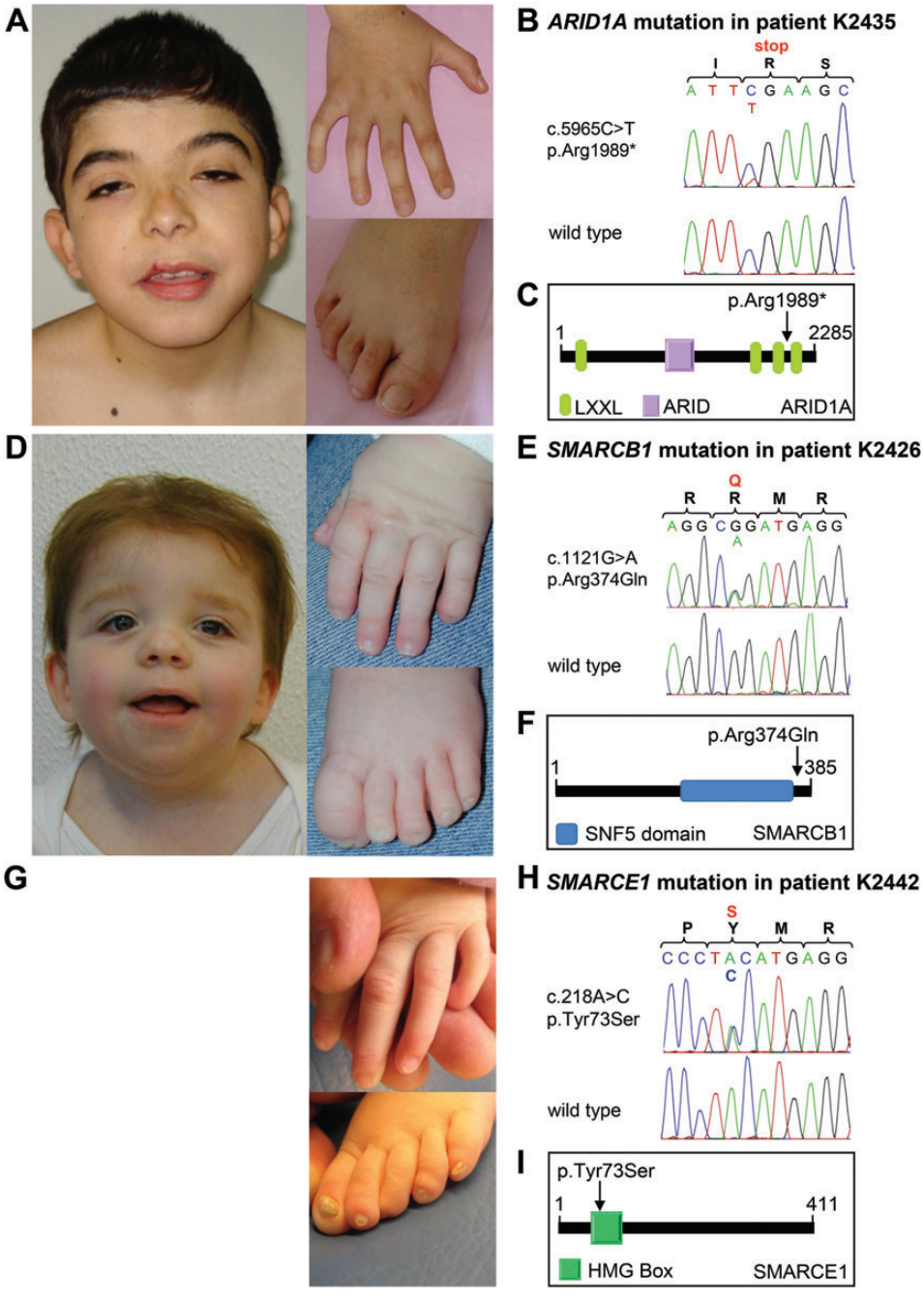

Figure 2. Clinical findings of CSS individuals with *ARID1A*, *SMARCB1* and *SMARCE1* mutations. (**A**) Individual K2435 with low frontal hairline, thick and arched eyebrows, ptosis, low-set ears, thin upper and full lower vermillion border. Brachytelephalangy with mild nail hypoplasia of all fingers and toes. (**B**) Electropherogram of the *ARID1A* mutation identified in individual K2435. (**C**) Schematic representation of the ARID1A protein; the p.Arg1989* mutation is located between two LXXL motifs. (**D**) Individual K2426 with sparse hair, hypertelorism, downward slanting palpebral fissures, short nose with anteverted nares, large mouth and low-set ears, nearly absent fifth fingernail and hypoplasia of toenails III and V. (**E**) Electropherogram of the *SMARCB1* mutation identified in individual K2426 compared with wild type. (**F**) Schematic representation of the SMARCB1 protein; the p.Arg374Gln mutation is located two amino acids downstream of the predicted SNF5 domain. (**G**) Individual K2442 with sparse hair, full eyebrows, broad nose, thin upper and full lower vermillion border, aplasia of the fifth fingernail and dystrophy of all toenails. (**H**) Electropherogram of the *SMARCE1* mutation identified in individual K2442 compared with wild type. (**I**) Schematic representation of the SMARCE1 protein; the p.Tyr73Ser mutation is located within the HMG box domain.

variant is predicted to be benign on PolyPhen (http://genetics.bwh.harvard.edu/pph2/) and lies within a non-conserved region. We therefore assume this variant to be likely non-pathogenic.

No pathogenic mutations were found in any of the candidate genes of the SWI/SNF complex that were included in the gene panel. We identified a missense variant in *CBL, SMARCD2* and *SMARCC1*, respectively, in three individuals with CSS, which were predicted to be damaging by PolyPhen (http://genetics.bwh.harvard.edu/pph2/) and, except for one, were not annotated in databases of human variation [Exome Variant

Downloaded from https://academic.oup.com/hmg/article/22/25/5121/575160 by guest on 15 March 2022

Server (http://evs.gs.washington.edu/EVS/), 1000 genomes (http://www.1000genomes.org/), dbSNP (http://www.ncbi.nlm.nih.gov/projects/SNP/)]. All of these variants were inherited from a healthy parent and were thus estimated to be not causative. However, we cannot completely exclude a causative role of these variants, for example as one inherited pathogenic allele in digenic inheritance.

Molecular karyotyping revealed deletions of the *ARID1B* gene in two individuals (K2428, K2438). In individual K2428, a partial *ARID1B* intragenic deletion of 58.5 kb comprising only exons 6–8 of the gene was identified. The deletion was confirmed and determined to be *de novo* by real-time polymerase chain reaction (PCR) (data not shown). Individual K2438 carries a larger deletion containing at least seven annotated genes: *ARID1B*, *ZDHHC14*, *SNX9*, *SYNJ2*, *SERAC1*, *GTF2H5* and *TULP4* (Table 1).

ARID1B mutations in individuals diagnosed with NCBRS

We examined nine individuals with a tentative diagnosis of NCBRS (Supplementary Material, Tables S1 and S2). In three of them (33%), we identified a missense mutation in *SMARCA2* (Table 1; Supplementary Material, Fig. S4), of which one (K2704 with the c.2639C>T mutation) was novel and proven to be *de novo*. The other two mutations were previously described in individuals with NCBRS and occurred *de novo* in individuals K2703 and K2704 and therefore, were assumed to be pathogenic (8). Interestingly, all *SMARCA2* missense mutations identified here are located in exon 18. We found mutations in *ARID1B* in three of the six remaining NCBRS individuals (50%). All of the *ARID1B* mutations were truncating (Table 1; Supplementary Material, Fig. S6), for two of them parental DNA was available for testing (K2703, K2706) and both mutations occurred *de novo*.

Additionally, we identified one *de novo* missense variant, c.1096C>T, in exon 9 of *SMARCB1* in an individual with NCBRS (K2588), reclassified as CSS. The putative mutation is not annotated in any database of human genomic variation, also including dbSNP (http://www.ncbi.nlm.nih.gov/projects/SNP/) and the Exome Variant Server (http://evs.gs.washington.edu/EVS/) and is predicted to be probably damaging with a PolyPhen (http://genetics.bwh.harvard.edu/pph2/) score of 1.0. The mutation substitutes the highly conserved arginine at position 366 within the SNF5 domain with cysteine (p.Arg366Cys; Fig. 2, Table 1).

DISCUSSION

The combination of whole-exome sequencing, NGS-based sequencing of SWI/SNF complex genes and molecular karyotyping identified causative dominant mutations in 60% (28/46) of the previously undescribed individuals studied here with a clinical diagnosis of either CSS or NCBRS.

PHF6 mutations in females lead to CSS phenotype

We identified *de novo* mutations in the X chromosomal gene *PHF6* in two female individuals with a convincing CSS phenotype (Table 1; Fig. 1). The 1-bp deletion c.677delG is predicted to cause a frame-shift and premature termination of the protein (p.Gly226Glufs*53), resulting in the loss of the second PHD-like zinc finger domain of the protein (Fig. 1F). This alteration most likely results in a loss-of-function of the protein, suggesting haploinsufficiency as the disease-causing mechanism. The other individual carries the *de novo* c.914G>T mutation, which affects a highly conserved cysteine within the second PHD-like zinc finger domain (p.Cys305Phe) providing additional evidence for the functional importance of this domain in PHF6 (Fig. 1C). It is of interest to note that mutations in *PHF6* have been previously reported in individuals with Borjeson-Forssman-Lehmann syndrome (BFLS, MIM 301900). The phenotype is well known in male individuals (13), but has been described only twice in females (14,15). The female phenotype in our two individuals in early infancy is clinically indistinguishable from CSS with ID, coarse facial features, thick and arched eyebrows with synophrys, large mouth with thick lower vermillion border, hypoplasia of distal phalanges, body hirsutism, sparse scalp hair and nail hypoplasia (Fig. 1). As the phenotypic spectrum of CSS is wide—especially in patients with *ARID1B* mutations—there is no specific clinical sign in early childhood, which helps to clinically separate both conditions. More characteristic phenotypic aspects of BFLS may not be evident in early childhood, but occur only later in adolescence or adulthood. Notably, both female individuals described here fulfilled the diagnostic criteria for CSS at the time of clinical evaluation.

PHF6 encodes the plant homeodomain (PHD) finger protein 6 (PHF6), expressed in the developing brain as well as in other embryonic tissues (16). Both identified mutations affect the second PHD-like zinc finger domain of the protein. This domain can directly interact with modified histones and is a common structure of chromatin remodeling proteins. Although no direct interaction of PHF6 with SWI/SNF complex proteins has been described, the phenotypic presentation in individuals with *PHF6* mutations suggests a functional link between PHF6 and the SWI/SNF complex and a common pathogenic pathway. It is well established that PHF6 interacts with the nucleosome remodeling and deacetylation (NuRD) complex implicated in chromatin remodeling (17). The NuRD complex is one of the four major types of ATP-dependent chromatin remodelers (18) and has similar functions as the SWI/SNF complex in transcriptional regulation through covalent histone modification during development. It will be an interesting task for future studies to identify the set of genes transcriptionally altered due to mutations in *PHF6* and the SWI/SNF complex genes *ARID1B, ARID1A, SMARCE1, SMARCB1* and *SMARCA2*. It wouldn't be surprising if these would be shown to converge on the same physiological pathways, demonstrating a common molecular pathogenesis of the SWI/SNF and PHF6-related disorders (19).

Mutations in *SMARCE1* and *SMARCB1* lead to severe CSS

So far, only one individual with a CSS-like phenotype and a missense mutation in *SMARCE1* (p.Tyr73Cys) has been published (3,20). Here, we describe the second individual with a *de novo* missense mutation affecting the same amino acid (p.Tyr73Ser) within the conserved high mobility domain (Fig. 2G–I), who displays typical findings of CSS. The affected individuals have severe ID (2/2), the typical craniofacial gestalt (2/2), hypertrichosis (1/2), and hypoplastic or absent fifth finger- and toenails associated with hypoplasia of other nails (2/2). In addition,

Downloaded from https://academic.oup.com/hmg/article/22/25/5121/575160 by guest on 15 March 2022

they are small for gestational age (2/2), have postnatal short stature (2/2) and severe microcephaly (2/2), complex congenital heart defects (2/2), feeding difficulties (2/2) and seizures (1/2). The hands of the individual described here were characterized by long and slender fingers with hypoplasia, especially of the second and aplasia of the fifth fingernails. All toenails were dystrophic and hypoplastic (Fig. 2G). The hands and feet were very similar to those of the individual published by Kosho *et al*. (20). This might help to clinically distinguish individuals eligible for *SMARCE1* testing. Loss-of-function mutations in *SMARCE1* cause isolated autosomal dominant multiple-spinal-meningioma disease (21), which was not noted in both individuals with *SMARCE1* mutation.

Exome sequencing in CSS individuals detected a single mutation in *SMARCB1* in a severely affected individual. Truncating mutations in *SMARCB1* have been identified in schwannomatosis (22). Only seven individuals with CSS and one individual with a Kleefstra syndrome-like phenotype with non-truncating *SMARCB1* mutations have yet been described (3,20,23). We here describe two additional *SMARCB1* mutations, one in an individual with CSS and one in an individual initially classified as NCBRS (retrospectively reclassified as CSS). These nine *SMARCB1* mutations (p.Arg377His (3), p.Lys364del in six individuals (3,11), p.Arg374Gln and p.Arg366Cys), are all located within exons 8 and 9 of the gene. These exons encode for the highly conserved sucrose/non-fermenting domain 5 (SNF5) of the protein. The phenotype of the individual with Kleefstra-like syndrome is different from the individuals with CSS with midface hypoplasia, upward slanting palpebral fissures and tongue protrusion, and might be explained by the different location and functional consequence of the mutation located close to the N-terminal part of the protein. Thus, mutations at different locations within the *SMARCB1* gene might lead to syndromic ID different from CSS.

In total, nine individuals with CSS with *SMARCB1* mutations are known. They present with developmental delay (7/7), the typical craniofacial gestalt (7/7), hypertrichosis (5/7) and hypoplastic or absent fifth finger- and toenails associated with hypoplasia of other nails (7/7). In addition, they are small for gestational age (3/7), have postnatal short stature (7/7) and microcephaly (6/7), congenital heart defects (3/7), small cerebellum (2/7), abnormal corpus callosum (4/5), diaphragmatic hernia (1/7), scoliosis (4/6), hearing impairment (5/5), feeding difficulties (7/7) and seizures (4/6).

ARID1B is the major gene for CSS and associated with a milder phenotype

In 32 individuals with CSS, a mutational screening was performed using Haloplex enrichment and NGS sequencing. Interestingly, only *ARID1B* mutations were identified in this cohort (13/32), which contained predominantly milder CSS phenotypes. In total, 16 mutations in *ARID1B* could be identified, including those detected by exome sequence and array analysis. Causative mutations in *ARID1B* were exclusively loss-of-function mutations (Table 1). We therefore suspect that only mutations leading to ARID1B haploinsufficiency cause a clinical phenotype. The phenotype of the *ARID1B* group is characterized by mild-to-moderate ID (16/16), a facial gestalt reminiscent of CSS (16/16) (Fig. 3), hypertrichosis (13/15) and hypoplastic, hardly ever absent fifth finger- and toenails (10/15) (Supplementary Material, Fig. S1). In addition, they are seldom small for gestational age (1/16) or have postnatal short stature (4/15) or microcephaly (2/16). Associated clinical anomalies, e.g. congenital heart defects (5/14), small cerebellum (0/14), abnormal corpus callosum (5/14), diaphragmatic hernia (0/16), scoliosis (2/13), hearing impairment (1/13), feeding difficulties (10/14) and seizures (4/16) were infrequently reported (specific clinical data were not available for every clinical sign).

Up to now, 64 individuals with CSS and *ARID1B* mutations have been published (including the individuals studied here) who represent the more severe end of the clinical spectrum of the *ARID1B* associated phenotype. In addition, Hoyer *et al*. reported on eight individuals with unspecific ID caused by *ARID1B* mutations, representing the mild end of the spectrum (4). Currently, we do not know why *ARID1B* mutations are associated with a milder phenotype compared to individuals carrying *SMARCB1* or *SMARCE1* mutations. Different functional consequences on the SWI/SNF complex by *ARID1B* haploinsufficiency and *SMARCB1*/*SMARCE1* missense mutations, which might exert a dominant-negative effect on other complex proteins, could explain the differences in the clinical phenotypes.

Intermediate CSS/NCBRS phenotypes make clinical distinction difficult

In addition to the group of individuals with clinically well-defined CSS, we included a clinically less characterized cohort of nine individuals with tentative diagnosis of NCBRS in our study. As frequently observed in a routine clinical setting, individuals were referred to us with the clinical diagnosis of NCBRS, but no photographs and detailed clinical data were available. Screening of this cohort for mutations revealed three missense mutations in the primary NCBRS gene *SMARCA2* and, interestingly, three truncating mutations in *ARID1B* and one missense mutation in *SMARCB1* (Table 1). In the remaining two individuals, no mutation within the SWI/SNF complex was identified pointing toward further genetic heterogeneity in NCBRS.

Clinical data and most photographs were finally obtained. These three individuals with *SMARCA2* mutations presented with a NCBRS phenotype consisting of sparse hair, short stature, seizures and prominent joints. Detailed clinical evaluation of the remaining individuals resulted in reclassification of the *ARID1B/SMARCB1* mutation carriers to the CSS phenotypic spectrum. The facial gestalt, especially in early childhood, may be very similar in both entities and does not allow discrimination between CSS and NCBRS. Sparse scalp hair was reported in both entities. The most distinguishing features are the hands and feet: Individuals with NCBRS do not manifest hypo- or aplasia of fifth finger- or toenail but swelling of interphalangeal joints. Tsurusaki *et al*. described one individual with a *SMARCA2* mutation who was previously diagnosed with CSS and reclassified as NCBRS (3,11), also demonstrating the described diagnostic dilemma. Thus, a small subset of individuals displays an intermediate CSS/NCBRS phenotype. Molecular testing is essential to establish the correct diagnosis in these individuals.

In summary, the molecular and clinical analyses of 46 undescribed individuals with either CSS or NCBRS presented here expand the molecular and clinical spectrum of these disorders and underscore the phenotypic and pathogenetic overlap.

Downloaded from https://academic.oup.com/hmg/article/22/25/5121/575160 by guest on 15 March 2022

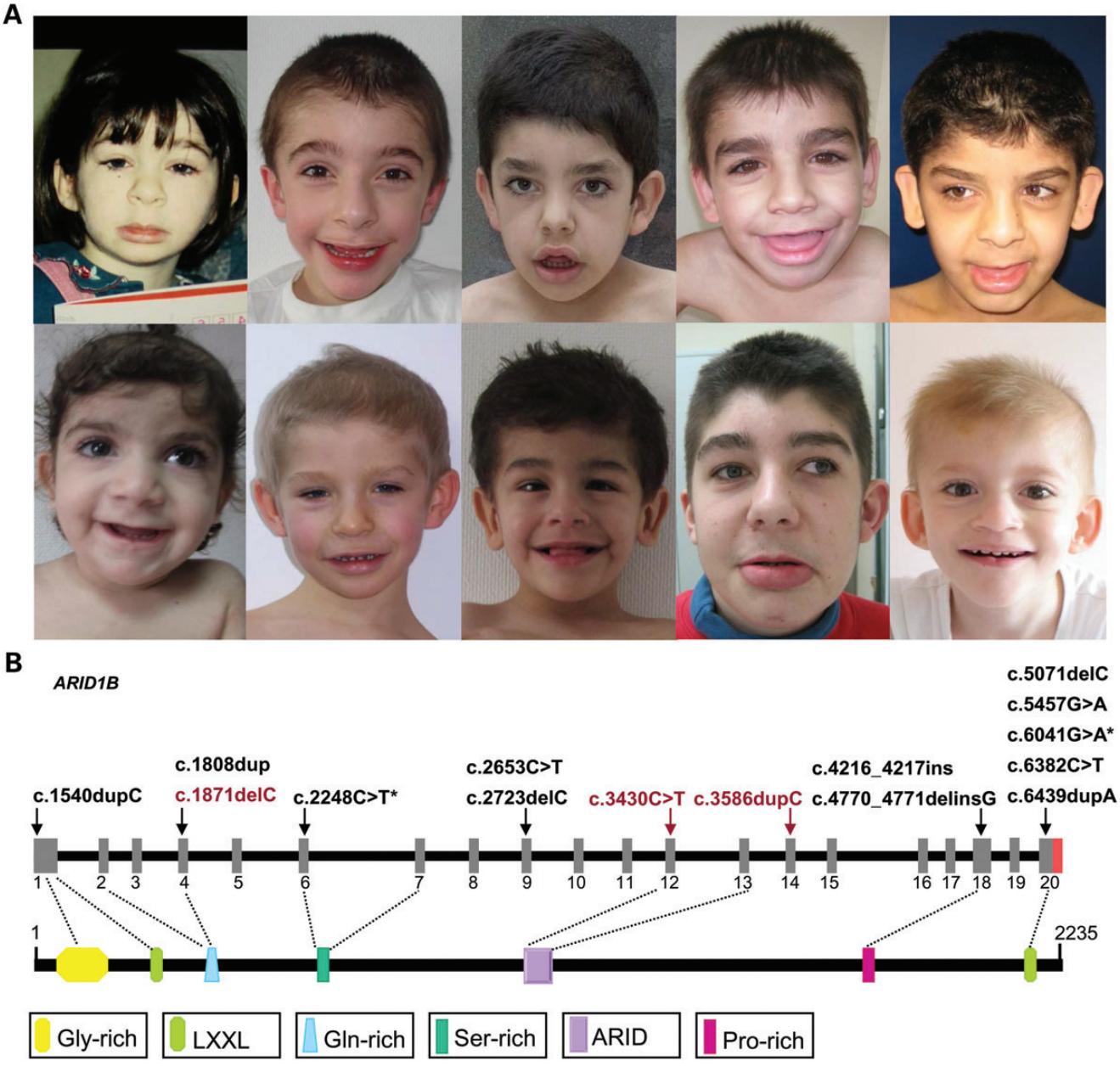

Figure 3. Craniofacial phenotype of individuals with *ARID1B* mutation. (**A**) Upper row from left to right: Individuals K2574, K2434, K2441, K2474 and K2471. Lower row from left to right: Individuals K2445, K2578, K2443, K2693 and K2428. (**B**) Schematic view of the ARID1B protein, all coding exons, and localization of identified *ARID1B* mutations. The mutations detected in CSS individuals are shown in black, and mutations identified in NCBRS individuals are depicted in red. Mutations marked with an asterisk were identified in two individuals.

Further studies will be needed to elucidate the underlying molecular pathogenesis in more detail and to shed light on the specific developmental mechanisms controlled by the relevant chromatin remodeling complexes.

MATERIALS AND METHODS

Subjects

Individuals with CSS or NCBRS and their parents were clinically assessed by experienced clinical geneticists. Clinical information pertinent to the diagnosis was provided by the parents or legal guardians for minors and by the evaluating authors. Detailed clinical data were evaluated by the authors (D.W., Y.A., H.K., B.A., K.B., A.C., K.Ch., O.C., J.C.C., K.D., N.E., B.G., T.O.G., M.K.-W., E.G.-N., J.H., G.H., E.K., P.Ö.S.-K., V.L.-G., S.L., F.Ö., A.Ra., S.T., G.E.U., C.Z., B.W.) and photographs of the face, hands and feet were available for all 37 individuals with the diagnosis CSS. For the nine individuals with a tentative diagnosis of NCBRS detailed clinical data were also obtained by the evaluating authors (M.T.D., E.G.-N., F.M., A.M., M.M.D., G.M., F.M.-P., A.Re., C.V., R.V.), but photographs and permission to publish them were limited. Detailed clinical data are listed in Tables 2 and 3 and Supplementary

Downloaded from https://academic.oup.com/hmg/article/22/25/5121/575160 by guest on 15 March 2022

Table 2. Clinical findings of mutation-positive CSS patients (part I)

	K2436	K2570	K2437	K2574	K2434	K2441	K2474	K2471	K2445	K2444	K2439
Gene/mutation	*PHF6*/c.914G>T	*PHF6*/c.677delG	*ARID1B*/ c.1540dupC	*ARID1B*/ c.1808dupG	*ARID1B*/ c.2248C>T	*ARID1B*/ c.2248C>T	*ARID1B*/ c.2692C>T	*ARID1B*/ c.2723delC	*ARID1B*/ c.4216_ 4217ins19bp	*ARID1B*/ c.4770_ 4771delinsG	*ARID1B*/ c.5071delC
Age at diagnosis (month)	33	96	30	n.r.	n.r.	48	84	1	15	36	36
Gender	f	f	f	f	m	m	m	m	f	f	f
consanguinity in parents	−	−	−	−	+	−	−	−	+	−	−
Age of mother at birth (year)	37	35	26	28	29	38	24	26	22	39	n.r.
Age of father at birth (year)	35	37	31	38	n.r.	44	38	28	29	42	n.r.
ID	+	+	+	+	+	+	++	+	+	+	+
Sat/walked independently (month)	>12/30	n.r./18	n.r./27	n.r./ 20	15/24	11/28	20/ 60	10/24	9/−	12 / 30	n.r./21
First words (month)	>36	13	36	n.r.	−	48	72	23	−	30	36
Hypotonia	+	−	+	+	+	n.r.	+	+	+	−	+
Seizures (year)	−	−	−	−	+	−	−	+	−	−	−
Vision problem	−	Nystagmus, strabismus	n.r.	−	−	n.r.	−	Strabismus, suspected optical atrophy	−	Nystagmus, strabismus	−
Hearing loss	−	−	n.r.	−	−	−	n.r.	−	mild (left ear)	−	n.r.
Frequent infections	+/− cystitis	−	+	−	+	−	−	+	−	−	−
Feeding problems	−	+	+	+	+	−	−	+	+	+	+
Behavioural anomalies	+/−	Anxiety	friendly, quiet, easily distracted, shy	−	−	−	+	Aggressive behaviour	−	−	−
Birth (weeks)	39	38	38	39	40	40	38	37	40	38	41
weight [g]/[SD]	3220/−0.5	2900/−0.7	2440/−1.74	2800/−1.3	2500/−2.5	3.025/−0.94	3050/−0.6	3200/0.22	3000/−1.1	3200/0.1	3700/0.3
length [cm]/[SD]	50/−0.3	49/−0.7	48/−1.04	48/−1.4	n.r.	48.6/−1.7	n.r.	49/−0.5	50/−0.8	n.r.	53/0.4
OFC [cm/SD]	35/0.3	33,5/−0.6	32/−0.23	34/−0.5	n.r.	37/1.34	n.r.	35/0.4	n.r.	n.r.	37/1.4
Age at examination (years)	10 5/6	9 11/12	12	n.r.	6 1/2	6 2/12	7	8 3/4	1 3/12	3	3
Height (cm)/(SD)	148.5/1.2	148/1.7	149/−0.27	160/0	117/−0.1	114.5/−0.67	107/−3.2	130/−0.88	77/0.54	93/−0.8	n.r.
OFC (cm/SD)	51/−0.9	54/1.4	52.4/−0.41	53,5/0	53/0.5	54/ 1.52	51/−1.2	56/2.1	46/0.15	49/−0.4	51/1.2
Craniofacial anomalies											
Coarse face	+	+	+	++	+	+	+	+	+	−	+
Low frontal hairline	−	+	+	+	+	+	+	+	+	−	+
Synophrys	+	+	−	+	−	−	+	+	+	−	−
Thick eyebrows	+, arched	+	+	+	+	+	+	+	+	+	+
Long eyelashes	−	−	+	+	+	+	+	+	+	+	−
Ptosis	−	−	−	+	+	−	−	−	+	−	−
Narrow palpebral fissures	−	−	−	−	−	−	+	+	−	−	−
Flat nasal bridge	−	+	−	+	+	−	+	−	+	+	−
Broad nose	−	+	−	+	+	+	+	+	+	−	+
Upturned nasal tip	+	−	−	−	−	−	−	−	−	+	−
Thick, anteverted alae nasi	+	−	+	+	−	+	+	+	+	+	+
Large mouth	+	+	+	++	+	+	+	+	+	+	+
Thin upper vermillion	+	−	−	+	+	n.r.	+	+	+	−	+
Thick lower vermillion	+	+	+	++	+	+	+	+	+	−	−
Macroglossia	−	−	−	+	−	+	+	+	+	−	+
Short philtrum	−	+	+	+	+	+	−	−	−	−	−
Long philtrum	+	−	−		−	−	+	+	+	−	+
Abnormal ears	+	−	+	−	−	+	+	low-set, large ear lobes	+	−	−
Cleft palate	−	−	n.r.	−	−	−	−	−	−	−	−
Skeletal anomalies											
A/Hypoplasia of distal phalanges V	+	+	+	+	+	Mild	Generally short distal phalanges	Brachymesophalangy V, generally short distal phalanges	+	−	Both 5. toes: distal phalanx hypoplastic, missing middle phalanx
Short metacarpals/ metatarsals	+	n.r.	n.r.	−	−	n.r.	n.r.	−	−	−	−

Continued

Downloaded from https://academic.oup.com/hmg/article/22/25/5121/575160 by guest on 15 March 2022

Downloaded from https://academic.oup.com/hmg/article/22/25/5121/575160 by guest on 15 March 2022

Table 2. *Continued*

	K2436	K2570	K2437	K2574	K2434	K2441	K2474	K2471	K2445	K2444	K2439
Prominent interphalangeal joints	+	+	n.r.	n.r.	+	−	+	−	+	−	−
Prominent distal phalanges	−	−	−	n.r.	+	−	+	−	+	−	−
Sandal gap	−	+	−	n.r.	−	n.r.	n.r.	n.r.	−	−	−
spinal anomalies	−	n.r.	n.r.	−	−	−	n.r.	n.r.	−	−	−
Delayed bone age	Advanced	−	n.r.	+(12 m)	−	n.r.	n.r.	+ (13 m)	n.r.	n.r.	n.r.
Scoliosis	−	+	−	−	−	n.r.	n.r.	n.r.	−	−	−
Internal anomalies											
cryptorchidism	Clitoris hypoplasia	/	/	/	−	+	−	Right	−	/	−
CHD	PDA	−	−	−(septal aneurysm with no shunt)	n.r.	−	−	Slight mitral insufficiency	−	n.r.	−
Ectodermal anomalies											
Body hirsutism	+	+	+	+	n.r.	+	+	+	+	+	−
Increased skin wrinkling	−	−	n.r.	+	n.r.	−	+	−	+	n.r.	−
Fetal finger pads	−	−	n.r.	+	−	+	+	−	−	n.r.	−
Sparse scalp hair	+	+	−	−	+	Mild	n.r.	+	+	+	+
Nail a/hypoplasia	Bil	+	left	+	−	Mild	−	−	+	n.r.	−
−Hands V	Bil	+	Bil	+	−	+	−	Short	+	n.r.	−
−Feet V	+	+		+	−	+	−	Short	−	n.r.	−
Delayed dentition	+	n.r.	+(13 mo)	++	n.r.	Abnormal dentition ("conic" teeth)	+	n.r.	+	n.r.	n.r.
Brain anomaliies						Hippocampal malrotation			+		
Small cerebellum	−	−	−	−	−	−	n.r.	−	−	−	−
Dandy–Walker anomaly	−	−	−	−	−	−	n.r.	−	−	−	−
Abnormal corpus callosum	−	−	−	−	−	+	n.r.	−	+	+	−
Others:	Streaky hyperpigmentation	Streaky hyperpigmentation	n.r.	Renal cysts	n.r.	Umbilical hernia	n.r.	Choroideal cysts in right and left lateral ventricle	n.r.	n.r.	n.r.

Table 3. Clinical findings of mutation positive CSS patients (part II)

	K2432	K2578	K2583	K2443	K2693	K2428	K2438	K2435	K2426	K2442
Gene/mutation	*ARID1B*/ c.5457G>A	*ARID1B*/ c.6041G>A	*ARID1B*/ c.6041G>A	*ARID1B*/ c.6382C>T	*ARID1B*/ c.6439dupA	*ARID1B*/ del6q25.3	*ARID1B*/ del6q25.3	*ARID1A*/ c.5965C>T	*SMARCB1*/ c.1121G>A	*SMARCE1*/ c.218A>C
Age at diagnosis (month)	96	84	10	48	84	15	72	117	4	30
Gender	m	m	m	m	m	M	m	m	M	f
consanguinity in parents	−	−	n.r.	+	−	−	no	−	−	−
Age of mother at birth (year)	38	29	n.r.	22	25	30	n.r.	29	37	18
Age of father at birth (year)	41	35	n.r.	24	26	32	n.r.	29	42	47
ID	+	+++	+	+	++	(++)	++	+	++	++
Sat/walked independently (month)]	12/24	9/25	late	24 / 30	10/20	9/34	n.r./31	n.r./>19	n.r./30	18 / 54
First words (month)	48	60	late	36	Absent speech	None, still babbling	65	12	−	No words, only vocalization
Hypotonia	+	+	n.r.	−	+	+	+	+	−	−
Seizures (year)	−	−	−	+	+	−	−	+	+	−
Vision problem	refractory error	−	−	Refraction error	Divergent strabismus	−	−	Strabismus	+	n.r.
Hearing loss	−	−	−	−	−	−	−	−	+	n.r.
Frequent infections	−	−	n.r.	−	−	+, sinopulmonary	−	−	+	+
Feeding problems	n.r.	−	n.r.	+	−	(++)	+	n.r.	++	++
Behavioural anomalies	−	+, hyperactivity	−	−	−	−	Rigid behavior	Hyperactivity	Hyperactivity	−
Birth (weeks)	38	39	39	33	40	39	42	38	33	38
Weight (g)/(SD)	2800/−1.2	3350/−0.3	3200/−0.7	1570/−1.3	2690/−2.1	2900/−0.65	3000/−1.7	n.r.	1720/−0.9	2200/−2,3
Length (cm)/(SD)	n.r.	51/−0.4	50/−0.8	n.r.	n.r.	49/0.23	n.r.	n.r.	42/−0.9	44 /−2,78
OFC (cm/SD)	n.r.	31/−3.3	35/−0.2	n.r.	n.r.	n.r.	n.r.	n.r.	30.5/−0.4	n.r.
Age at examination (year)	8	4	10	4	15	$1\frac{1}{4}$	17	9 3/4	4 1/4	3 1/4
Height (cm)/(SD)	108/−3.8	99/−1.4	129/−1.8	90/−3.6	155,5/0	75/−1.62	153.5/−3.4	130/−1.6	92/−3.35	86/−3.67
OFC (cm/SD)	53/0.1	51,5/mean	52/−0.8	48/−2.5	54,5/−0.5	42/−2.94	57.5/0.8	52.8/−0.3	46/−3,17	43/−4.6
Craniofacial anomalies										
Coarse face	+	+	+	+	+	+	+	+	+	+
Low frontal hairline	+	+	+	−	+	−	n.r.	+	+	+
Synophrys	−	−	−	−	−	−	−	−	−	−
Thick eyebrows	+	+	−	+	+	−	+	+	+	+
Long eyelashes	+	+	+	+	−	+	+	+	+	+
Ptosis	+	+	−	−	−	−	−	+	+	+
Narrow palpebral fissures	−	+	−	−	−	−	−	−	−	−
Flat nasal bridge	+	+	−	+	−	+	−	+	+	+
Broad nose	+	+	+	+	+	+ (broad nasal tip)	−	+	+	+

Continued

Downloaded from https://academic.oup.com/hmg/article/22/25/5121/575160 by guest on 15 March 2022

Downloaded from https://academic.oup.com/hmg/article/22/25/5121/575160 by guest on 15 March 2022

Table 3. *Continued*

	K2432	K2578	K2583	K2443	K2693	K2428	K2438	K2435	K2426	K2442
Upturned nasal tip	−	+	−	+	+	−	+	+	−	−
Thick, anteverted alae nasi	+	+	+	+	+	+	+	−	−	+
Large mouth	+	+	+	+	+	+	+	+	+	+
Thin upper vermillion	+	−	−	−	+	−	−	−	+	+
Thick lower vermillion	+	+	+	−	+	−	+	+	+	+
Macroglossia	−	−	−	−	−	−	+	+	+	−
Short philtrum	−	+	−	−	−	−	−	+	−	+
Long philtrum	+	−	−	−	+	+	−	−	−	−
Abnormal ears	−	Large	+	+	+	+	−	+	Small auditory canal	+
Cleft palate	−	−	−	−	−	−	−	−	−	Suspicion
Skeletal anomalies							+			
A/Hypoplasia of distal phalanges V	+	+	+	+	+	+	Generally short distal phalanges	−	+, 2–4	+
Short metacarpals/ metatarsals	n.r.	−	−	−	−	IV − V	−	+	n.r.	n.r.
Prominent interphalangeal joints	+	+	−	−	+	−	−	+	n.r.	n.r.
Prominent distal phalanges	+	−	+	−	+	−	−	−	−	−
Sandal gap	−	+	+	−	+	+	−	+	+	+
Spinal anomalies	−	−	n.r.	−	n.r.	−	−	−	n.r.	n.r.
Delayed bone age	+	−	n.r.		n.r.	n.r.	+	+	++	+
Scoliosis	+	−	−	+	−	−	−	−	+	−
Internal anomalies										
Cryptorchidism	−	−	−	+	+	+	−	+	+	/
CHD	−	PFO	−	ASD	−	AVSD, secundum ASD	ASD	−	VSD, ASD, pulmonic stenosis	ASD, dextropositio cordis, slightly pulmonal hypertension, enlarged right ventricle
Ectodermal anomalies										
Body hirsutism	+	+	+	+	+	−	+	+	+	n.r.
Increased skin wrinkling	−	−	+	n.r.	−	+, hands	−	−	−	−
Fetal finger pads	−	n.r.	+	n.r.	−	+	−	−	−	−
Sparse scalp hair	+	+	+	+	−	++	+	−	+	+
Nail a/hypoplasia	+	+	+	Hypoplasia of toe nails	+	−	+	+	Bil	+
− Hands V	+	−	+	+	+	(−)	+	−	Bil	+
− Feet V	+	+	+	+	+	(−)	+	−	bil	+

Delayed dentition	+	n.r.	n.r.	+	n.r.	+	+	n.r.	+	n.r.
Brain anomalies			n.r.	n.r.						
Small cerebellum	−	−	n.r.	−	−	−	−	−	−	+
Dandy – Walker anomaly	−	−	n.r.	−	−	−	−	−	−	+
Abnormal corpus callosum	+	−	n.r.	+	−	−	−	+	+	+
Others:	Umbilical hernia	−	n.r.	n.r.	n.r.	Umbilical hernia, nephrolithiasis	n.r.	Double ureter, diabetes mellitus II	Pylorus stenosis	n.r.

Material, Tables S1 and S2. Clinical photographs are depicted in Figures 1 and 2 and Supplementary Material, Figures S1–6.

We obtained a written informed consent from the families of the index individuals for participation in this study. The study was performed according to the Declaration of Helsinki protocols and was approved by the local institutional review board (ethical votum 12-5089-BO for CRANIRARE and 08-3663 for MRNET). Blood samples were collected from the affected individuals and their parents and DNA was extracted from peripheral blood lymphocytes by standard extraction procedures.

Exome sequencing

Genomic library preparation

Exome sequencing was performed on DNA from individuals K2437, K2426, K2442, K2436 and their eight parents and on DNA from individuals K2434 and K2435 for whom parental DNA was not available. Exome capture was performed on DNA from individuals K2434 and K2435 with the NimbleGen SeqCap EZ Human Exome Library SR KIT (Roche NimbleGen, Waldkraiburg, Germany). Five microgram of genomic DNA was fragmented by nebulization using a nebulizer device (Invitrogen, Darmstadt, Germany) following the manufacturer's instructions. The fragmented DNA was purified using a QIAquick PCR Purification column (Qiagen, Hilden, Germany) and quantified on a Nanodrop Photometer. Genomic libraries were prepared using the Illumina Paired End Sample Prep kit following the manufacturer's instructions (Illumina, San Diego, CA, USA), which includes a size selection of DNA fragments in the size range of ~200–400 bp on a 2% agarose gel. Exome enrichment was performed with 1 μg of the adapter-ligated DNA sample following the manufacturer's instructions.

NimbleGen SeqCap EZ Human Exome Library v2.0 was used to capture the exomes of the samples K2437, K2426, K2442 and K2436 as described previously (24). Briefly, one microgram genomic DNA was fragmented by use of a Covaris S220 (CovarisInc, Woburn, MA, USA). Libraries were generated using the TruSeq Sample Preparation Kit v2 (Illumina) following the low-throughput and gel-free method protocols. Sequencing of enriched DNA fragments was performed on an Illumina HiSeq2000 platform using the paired-end sequencing protocol with a read length of 101 bp each.

Data analyses

Sequence reads were mapped to the human genome reference assembly GRCh37 (25) using BWA version 0.5.9-r18-dev (26); PCR duplicates were removed using Picard 1.63; for indel realignment, quality recalibration and variant calling, the Genome Analysis Toolkit version 1.4-33-g051b450 was used (27). UnifiedGenotyper was used for both SNP and indel calling. We obtained in between 3 and 3.5 Gbp of non-duplicate on-target sequence for each sample captured by use of the SeqCap EZ Human Exome Library v2.0 resulting in 85% of the 44 Mbp target sequence covered at least 20-fold. For both samples captured with the SeqCap EZ Human Exome Library SR kit, we obtained 0.3 Gbp on target sequence. Variants were annotated with custom software using the ENSEMBL gene annotation track v63 and kept if they were non-synonymous,

Downloaded from https://academic.oup.com/hmg/article/22/25/5121/575160 by guest on 15 March 2022

indel, missense, nonsense or in the vicinity of a splice site (within 4 bp of an exon/intron border).

Filtering

We filtered out all variants that occurred in the in-house database or dbSNP 135 (but not filtering those marked as 'clinical', 'precious' or 'contained in a locus-specific database') and those occurring in mucin genes. The in-house database contained exomes of 105 healthy probands, including the eight parents of individuals K2437, K2426, K2442 and K2436. To identify *de novo* mutations, we set the threshold for the variant quality score (as reported by UnifiedGenotyper) to 200. After filtering, a total of 201 sequence variations were identified in the exomes from all six affected individuals. On average, 33 candidate genes with a sequence variation were identified per sample. We reassessed the sequence alterations of four candidate genes of the SWI/SNF complex by Sanger sequencing and confirmed the *de novo* mutations in all of them.

We used PolyPhen (http://genetics.bwh.harvard.edu/pph2/) to predict the possible impact of missense mutations on the structure and function of a protein.

Haloplex target enrichment

Libraries of all coding exons and exon–intron boundaries of the known CSS genes *ARID1A* (NM_006015.4), *ARID1B* (NM_020732.3), *SMARCA2* (NM_003070.3), *SMARCA4* (NM_001128849.1), *SMARCB1* (NM_003073.3), and *SMARCE1* (NM_003079.4), as well as the candidate genes *ARID2* (NM_152641.2), *SMARCC1* (NM_003074.3), *SMARCC2* (NM_003075.3), *SMARCD1* (NM_003076.4), *SMARCD2* (NM_001098426.1), *SMARCD3* (NM_003078.3), *ACTL6A* (NM_004301.3), *ACTL6B* (NM_016188.4), *PBRM1* (NM_018313.4), *BRD7* (NM_001173984.2), *PRMT5* (NM_006109.3), *SMARCA1* (NM_003069.3), *SMARCA5* (NM_003601.3), *HELLS* (NM_018063.3), *CBL* (NM_005188.3), *C7orf11* (NM_138701) and *SHOC2* (NM_007373.3) were prepared from 200 ng of genomic DNA from 41 index individuals using a customised HaloPlex target enrichment kit (Agilent technologies, Santa Clara, USA), following the manufacturer's protocol. The resulting fragment libraries were sequenced from both ends (100 bp paired-end sequencing) using the Illumina HiSeq 2000 running Version3 chemistry (Illumina, San Diego, USA). Candidate genes were chosen according to structural homology, a functional relationship, or if known to cause an overlapping phenotype. The total target region size was 188 589 bp.

Validation by Sanger sequencing

Relevant variants were re-sequenced by Sanger sequencing. The affected exons of *ARID1B, SMARCA2, SMARCB1, SMARCD2*, *SMARCC1, CBL, PHF6* and *ARID1A* were amplified from DNA of the affected individuals and—if available—their parents by PCR, performed according to the standard procedures, and were sequenced using the BigDye Terminator method on an ABI 3010xl or ABI 3100 sequencer. Sequencing data were analyzed using the Geneious Pro (5.6.4.) software (Biomatters Ltd, New Zealand) or the FinchTV software (Geospiza, Seattle, USA). All primers for amplification and sequencing were selected with ExonPrimer and were ordered from Biomers (Ulm, Germany) or IDT (Leuven, Belgium; primer sequences are available on request).

Molecular karyotyping

A genome-wide copy number microarray analysis was performed using the Affymetrix 6.0 SNP array in individual K2438 and the CytoScanHD array in individual K2428 (Affymetrix, Santa Clara, CA, USA) according to the manufacturer's instructions. Data analysis was carried out using the Affymetrix Chromosome Analyse Suite (ChAS v1.2 or v2.0), and the data interpretation was based on the February 2009 human genome sequence assembly (GRCh37/hg19). Conspicuous regions were compared with known CNVs, as provided by the Database of Genomic Variants (http://projects.tcag.ca/variation/). Particular attention was paid to the genes that code for known components of the SWI/SNF complex.

Quantitative real-time PCR

The presence of the *ARID1B*-intragenic deletion in individual K2438 was confirmed by a quantitative real-time PCR assay using the Roche Universal ProbeLibrary System. Part of exon 7 of *ARID1B* (chr6:157454217-157454286) was amplified with primers ARID1B_left: 5′-GACAGGACCATCCATGTCG-3′ and ARID1B_right: 5′-CTGAAAGCTACTGATTCCAGCA-3′, and detected with the universal probe 2. As an internal control, an assay for the AS-SRO on chromosome 15 was used (28). The analysis was performed on the LightCycler 480 (Roche).

SUPPLEMENTARY MATERIAL

Supplementary Material is available at *HMG* online.

ACKNOWLEDGEMENTS

We thank the probands and their families for participating in this study. We also thank Karin Boss for critically reading the manuscript and Daniela Falkenstein, Sabine Kaya and Lars Maßhöfer for excellent technical assistance.

Conflict of Interest Statement. None declared.

FUNDING

This work was part of the CRANIRARE-2 Network funded by the German Federal Ministry of Education and Research (BMBF) (01GM1211A to B.W., 01GM1211B to D.W.), the TUBITAK (112S398 to H.K.) and ERARE-ANR CraniRare to S.L. This work was also funded by a grant (MRNET) from the German Federal Ministry of Education and Research (01GS08167 to D.W.), by DFG grants (BO 1955/2-3 and WU 314/6-2 to S.B. and D.W.) and by the Volkswagen Foundation (ref 86042 to A.W.). The biobank "Cell lines and DNA bank of Rett syndrome, X linked Mental Retardation and other genetic diseases", member of the Telethon Network of Genetic Biobanks (project no. GTB12001), funded by Telethon Italy, provided us with specimens.

Downloaded from https://academic.oup.com/hmg/article/22/25/5121/575160 by guest on 15 March 2022

REFERENCES

1. Liu, N., Balliano, A. and Hayes, J.J. (2011) Mechanism(s) of SWI/SNF-induced nucleosome mobilization. *Chembiochem.*, **12**, 196–204.
2. Santen, G.W., Aten, E., Sun, Y., Almomani, R., Gilissen, C., Nielsen, M., Kant, S.G., Snoeck, I.N., Peeters, E.A., Hilhorst-Hofstee, Y. *et al.* (2012) Mutations in SWI/SNF chromatin remodeling complex gene ARID1B cause Coffin–Siris syndrome. *Nat. Genet.*, **44**, 379–380.
3. Tsurusaki, Y., Okamoto, N., Ohashi, H., Kosho, T., Imai, Y., Hibi-Ko, Y., Kaname, T., Naritomi, K., Kawame, H., Wakui, K. *et al.* (2012) Mutations affecting components of the SWI/SNF complex cause CoffinSiris syndrome. *Nat. Genet.*, **44**, 376–378.
4. Hoyer, J., Ekici, A.B., Endele, S., Popp, B., Zweier, C., Wiesener, A., Wohlleber, E., Dufke, A., Rossier, E., Petsch, C. *et al.* (2012) Haploinsufficiency of ARID1B, a member of the SWI/SNF-a chromatin-remodeling complex, is a frequent cause of intellectual disability. *Am. J. Hum. Genet.*, **90**, 565–572.
5. Coffin, G.S. and Siris, E. (1970) Mental retardation with absent fifth fingernail and terminal phalanx. *Am. J. Dis. Child.*, **119**, 433–439.
6. Fleck, B.J., Pandya, A., Vanner, L., Kerkering, K. and Bodurtha, J. (2001) Coffin–Siris syndrome: review and presentation of new cases from a questionnaire study. *Am. J. Med. Genet.*, **99**, 1–7.
7. Schrier Vergano, S., Santen, G., Wieczorek, D., Wollnik, B., Matsumoto, N. and Deardorff, M.A. (2013) Coffin–Siris syndrome. In: Pagon, R.A., Adam, M.P., Bird, T.D. *et al.* (eds), *Gene Reviews [Internet]*. Seattle (WA): University of Washington, 1993–2013.
8. Van Houdt, J.K., Nowakowska, B.A., Sousa, S.B., van Schaik, B.D., Seuntjens, E., Avonce, N., Sifrim, A., Abdul-Rahman, O.A., van den Boogaard, M.J., Bottani, A. *et al.* (2012) Heterozygous missense mutations in SMARCA2 cause Nicolaides–Baraitser syndrome. *Nat. Genet.*, **44**, 445–449. S441.
9. Nicolaides, P. and Baraitser, M. (1993) An unusual syndrome with mental retardation and sparse hair. *Clin. Dysmorphol.*, **2**, 232–236.
10. Sousa, S.B., Abdul-Rahman, O.A., Bottani, A., Cormier-Daire, V., Fryer, A., Gillessen-Kaesbach, G., Horn, D., Josifova, D., Kuechler, A., Lees, M. *et al.* (2009) Nicolaides–Baraitser syndrome: Delineation of the phenotype. *Am. J. Med. Genet. A*, **149A**, 1628–1640.
11. Tsurusaki, Y., Okamota, N., Ohashi, H., Mizuno, S., Matsumoto, N., Makita, Y., Fukuda, M., Isidor, B., Perrier, J., Aggarwal, S. *et al.* (2013) Coffin–Siris syndrome is a SWI/SNF complex disorder. *Clin. Genet*, doi: 10.1111/cge.12225.
12. Ye, K., Schulz, M.H., Long, Q., Apweiler, R. and Ning, Z. (2009) Pindel: a pattern growth approach to detect break points of large deletions and medium sized insertions from paired-end short reads. *Bioinformatics*, **25**, 2865–2871.
13. Lower, K.M., Turner, G., Kerr, B.A., Mathews, K.D., Shaw, M.A., Gedeon, A.K., Schelley, S., Hoyme, H.E., White, S.M., Delatycki, M.B. *et al.* (2002) Mutations in PHF6 are associated with Börjeson–Forssman–Lehmann syndrome. *Nat. Genet.*, **32**, 661–665.
14. Berland, S., Alme, K., Brendehaug, A., Houge, G. and Hovland, R. (2011) PHF6 deletions may cause Borjeson–Forssman–Lehmann syndrome in females. *Mol. Syndromol.*, **1**, 294–300.
15. Crawford, J., Lower, K.M., Hennekam, R.C., Van Esch, H., Mégarbané, A., Lynch, S.A., Turner, G. and Gécz, J. (2006) Mutation screening in Borjeson–Forssman–Lehmann syndrome: identification of a novel de novo PHF6 mutation in a female patient. *J. Med. Genet.*, **43**, 238–243.
16. Voss, A.K., Gamble, R., Collin, C., Shoubridge, C., Corbett, M., Gécz, J. and Thomas, T. (2007) Protein and gene expression analysis of Phf6, the gene mutated in the Börjeson–Forssman–Lehmann Syndrome of intellectual disability and obesity. *Gene Expr. Patterns*, **7**, 858–871.
17. Todd, M.A. and Picketts, D.J. (2012) PHF6 interacts with the nucleosome remodeling and deacetylation (NuRD) complex. *J. Proteome Res.*, **11**, 4326–4337.
18. Clapier, C.R. and Cairns, B.R. (2009) The biology of chromatin remodeling complexes. *Annu. Rev. Biochem.*, **78**, 273–304.
19. Gao, H., Lukin, K., Ramírez, J., Fields, S., Lopez, D. and Hagman, J. (2009) Opposing effects of SWI/SNF and Mi-2/NuRD chromatin remodeling complexes on epigenetic reprogramming by EBF and Pax5. *Proc. Natl Acad. Sci. USA*, **106**, 11258–11263.
20. Kosho, T., Okamoto, N., Ohashi, H., Tsurusaki, Y., Imai, Y., Hibi-Ko, Y., Kawame, H., Homma, T., Tanabe, S., Kato, M. *et al.* (2013) Clinical correlations of mutations affecting six components of the SWI/SNF complex: detailed description of 21 patients and a review of the literature. *Am. J. Med. Genet. A.*, **161**, 1221–1237.
21. Smith, M.J., O'Sullivan, J., Bhaskar, S.S., Hadfield, K.D., Poke, G., Caird, J., Sharif, S., Eccles, D., Fitzpatrick, D., Rawluk, D. *et al.* (2013) Loss-of-function mutations in SMARCE1 cause an inherited disorder of multiple spinal meningiomas. *Nat. Genet.*, **45**, 295–298.
22. Swensen, J.J., Keyser, J., Coffin, C.M., Biegel, J.A., Viskochil, D.H. and Williams, M.S. (2009) Familial occurrence of schwannomas and malignant rhabdoid tumour associated with a duplication in SMARCB1. *J. Med. Genet.*, **46**, 68–72.
23. Kleefstra, T., Kramer, J.M., Neveling, K., Willemsen, M.H., Koemans, T.S., Vissers, L.E., Wissink-Lindhout, W., Fenckova, M., van den Akker, W.M., Kasri, N.N. *et al.* (2012) Disruption of an EHMT1-associated chromatin-modification module causes intellectual disability. *Am. J. Hum. Genet.*, **91**, 73–82.
24. Czeschik, J.C., Voigt, C., Alanay, Y., Albrecht, B., Avci, S., Fitzpatrick, D., Goudie, D.R., Hehr, U., Hoogeboom, A.J., Kayserili, H. *et al.* (2013) Clinical and mutation data in 12 patients with the clinical diagnosis of Nager syndrome. *Hum. Genet.*, **132**, 885–898.
25. Church, D.M., Schneider, V.A., Graves, T., Auger, K., Cunningham, F., Bouk, N., Chen, H.C., Agarwala, R., McLaren, W.M., Ritchie, G.R. *et al.* (2011) Modernizing reference genome assemblies. *PLoS Biol.*, **9**, e1001091.
26. Li, H. and Durbin, R. (2009) Fast and accurate short read alignment with Burrows–Wheeler transform. *Bioinformatics*, **25**, 1754–1760.
27. DePristo, M.A., Banks, E., Poplin, R., Garimella, K.V., Maguire, J.R., Hartl, C., Philippakis, A.A., del Angel, G., Rivas, M.A., Hanna, M. *et al.* (2011) A framework for variation discovery and genotyping using next-generation DNA sequencing data. *Nat. Genet.*, **43**, 491–498.
28. Ronan, A., Buiting, K. and Dudding, T. (2008) Atypical Angelman syndrome with macrocephaly due to a familial imprinting center deletion. *Am. J. Med. Genet. A*, **146A**, 78–82.

Downloaded from https://academic.oup.com/hmg/article/22/25/5121/575160 by guest on 15 March 2022